

GENERATION OF SUB-PICOSECOND X-RAY PULSES AT BESSY-II

S. Khan, BESSY-II, Rudower Chaussee 5, 12489 Berlin, Germany

Abstract

Two methods to generate sub-picosecond x-ray pulses using the electron beam of the BESSY-II storage ring in combination with a femtosecond laser are discussed:

(1) Thomson scattering of laser pulses crossing electron bunches at a small angle.

(2) Energy-modulation of a short region within an electron bunch interacting with the laser in an undulator, and subsequent emission of synchrotron radiation.

1 INTRODUCTION

The technology of visible laser pulses below 100 fs duration is well established, whereas pulses produced by VUV and x-ray sources are in general much longer than 1 ps.

This paper describes two methods to generate sub-picosecond x-ray pulses using the electron beam of a third-generation synchrotron light source in combination with a femtosecond laser.

A suitable laser is a Ti:sapphire system based on chirped pulse amplification (CPA) with a wavelength of 800 nm, a typical pulse duration of 100 fs FWHM (43 fs rms) and an average power of a few Watt.

All estimates are based on the storage ring parameters of the high-brilliance synchrotron light source BESSY-II currently under construction at Berlin-Adlershof [1]. The following modes of operation are considered:

- A beam energy of 1700 MeV or 900 MeV.
- 100 mA in 320 bunches or 10 mA in a single bunch.

2 THOMSON SCATTERING

The generation of sub-picosecond x-ray pulses by crossing a femtosecond laser at a right angle with a 50 MeV electron beam has been successfully demonstrated at the Advanced Light Source (ALS) at Berkeley [2]. An analogous experiment at BESSY-II using the 50 MeV injection microtron is presently not considered because of the comparatively low beam current from this machine.

Generating x-ray photons using the BESSY-II storage ring beam at higher energy requires small crossing angles (10-50 mrad). Although the scattering rate is strongly reduced at small angles, there are several advantages to this configuration:

- Extremely short x-ray pulses (\approx laser pulse length).
- Small source point (high brilliance).
- Small divergence of the x-ray beam (high brilliance).
- Small electron divergence (little spectral broadening).

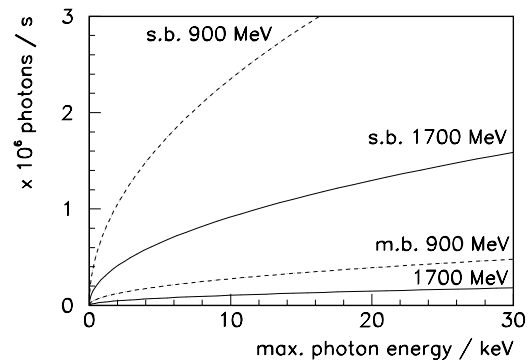


Figure 1: Scattering rate as function of the endpoint of the scattered photon spectrum for singlebunch (s.b.) and multibunch (m.b.) operation of the BESSY-II storage ring at 900 MeV and at 1700 MeV.

2.1 Properties of Thomson Scattered Photons

In a right-angle geometry, the transit time of the laser pulse through the electron bunch adds to the duration of the scattered photon pulse. When the laser and the electron beam are almost parallel, the x-ray pulse duration is essentially given by the laser pulse length.

The endpoint of the scattered photon spectrum is

$$E'_{\max} = 2\gamma^2 E(1 - \cos \alpha), \quad (1)$$

where E is the laser photon energy, α is the crossing angle, and γ is the electron Lorentz factor. For a laser pulse with N_γ photons crossing a bunch with N_e electrons, an upper limit for the scattering rate is

$$N = \frac{N_\gamma N_e \sigma_{\text{Th}}}{2\pi \sigma_y \sigma_z} \cdot \frac{1 - \cos \alpha}{\sin \alpha} \quad (\text{for } \sigma_x \ll \sigma_z, \beta = 1). \quad (2)$$

Here, $\sigma_{\text{Th}} = 6.7 \cdot 10^{-29} \text{ m}^2$ is the Thomson cross section, σ_z is the rms bunch length, σ_x is the bunch size in the crossing plane, and σ_y is the bunch size perpendicular to it. Equation 2 holds for a transverse laser size being small compared to bunch dimensions. Half of the N photons are scattered into a cone of opening angle $2/\gamma$.

The photon scattering rate N as function of the endpoint energy E' is shown in figure 1 for different modes of operation. Singlebunch mode at a low beam energy is clearly favorable.

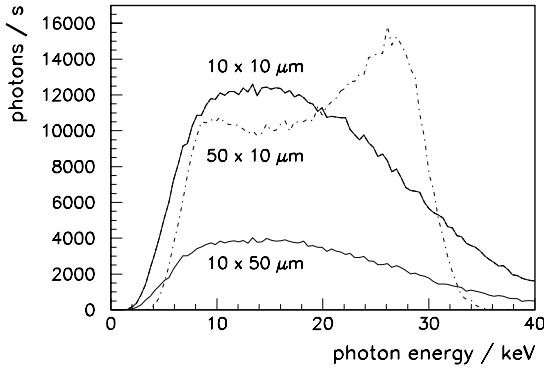


Figure 2: Spectra of Thomson scattered photons for different laser waists (horizontal \times vertical rms size).

2.2 Simulation of the Thomson Scattering Process

In order to study the Thomson scattering process in more detail, a Monte Carlo simulation was performed. Event by event, the spatial and angular photon coordinates within a Gaussian laser pulse, the location of the interaction within the electron bunch, the angular electron coordinates, the polar and the azimuthal scattering angle were randomly chosen. For horizontal crossing, the following observations were made:

A small laser waist (e.g. $10 \times 10 \mu\text{m}$, figure 2) yields a large scattering rate, but the spectrum is broadened due to the angular divergence of the laser. Increasing the vertical waist size only reduces the rate, whereas increasing the horizontal waist reduces the broadening effect without affecting the rate.

Taking 85-100% of the endpoint energy into account, the scattered photon brilliance defined as

$$B = \frac{\text{photons}/(15\% \text{bw s})}{150 \cdot 2\sigma_x 2\sigma_y 2\sigma'_x 2\sigma'_y} \left[\frac{\text{photons}}{0.1\% \text{bw mm}^2 \text{mrad}^2 \text{s}} \right] \quad (3)$$

is shown in figure 3 for singlebunch operation. Here, $\sigma_{x,y}$ is the electron beam size, while $\sigma'_{x,y}$ is the observed rms angular spread of photons within a 15% bandwidth.

3 LASER-ELECTRON INTERACTION

The second method discussed in this paper and proposed by [3] is based on a short laser pulse of wavelength λ_L travelling together with an electron bunch of Lorentz factor γ through an undulator of period length λ_u . If the undulator parameter K satisfies the resonance condition

$$(1 + K^2/2)\lambda_u = 2\gamma^2\lambda_L, \quad (4)$$

the laser produces a short region within the bunch, where electrons have gained or lost energy, depending on their phase relative to the laser field. A transverse displacement of these energy-modulated electrons by dispersion in the next bending magnet or undulator allows to extract a short synchrotron radiation pulse.

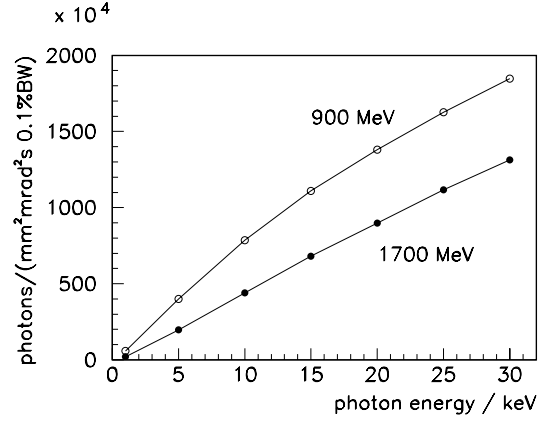


Figure 3: Brilliance of Thomson scattered photons as defined in equation 3 for single-bunch mode.

3.1 Estimates

Among the to-date specified insertion devices for BESSY-II, only the W/U-125 with $N_u = 32$ periods of length $\lambda_u = 125 \text{ mm}$ and $K \leq 12.8$ satisfies equation 4, provided a Ti:Sa CPA laser with second harmonic generation is employed i.e. $\lambda_L = 400 \text{ nm}$, which leads to $K = 11.8$.

Following [3], the amplitude for an energy-modulation ΔE is given by

$$(\Delta E)^2 = 4\pi\alpha E_L A_L \frac{K^2/2}{1 + K^2/2} \cdot \frac{\Delta\omega_L}{\Delta\omega_u}, \quad (5)$$

where $E_L = 3.1 \text{ eV}$ is the laser photon energy and A_L is the energy per laser pulse. For a typical laser pulse length of 100 fs FWHM (or $\tau_L = 43 \text{ fs}$ rms), the laser/undulator bandwidth ratio is $\Delta\omega_L/\Delta\omega_u \approx 0.3$. Demanding a modulation amplitude of 2% of the beam energy, equation 5 leads to $A_L = 2.2 \text{ mJ}$ for a beam energy of 1700 MeV. Consequently, the repetition rate f is 0.45 kHz for an average laser power of 1 W.

The number of energy-modulated electrons per second is

$$N = f \eta N_e \tau_L / \tau_e, \quad (6)$$

where $\eta \approx 0.2$ [3] accounts for the fact that only a fraction of the electrons acquire a sufficiently large energy deviation. Table 1 summarizes the result for multibunch mode ($N_e = 1.6 \cdot 10^9$ electrons/bunch and rms bunch length $\tau_e = 17 \text{ ps}$) at 1900 MeV and at 900 MeV. Singlebunch mode is not considered, because the background from previous interactions would limit f to the radiation damping rate (120 Hz at 1700 MeV, 20 Hz at 900 MeV).

E / MeV	A_L / mJ	f / kHz	N / s^{-1}
1700	2.2	0.45	$3.6 \cdot 10^8$
900	0.6	1.6	$1.3 \cdot 10^9$

Table 1: Estimates on energy modulation for multibunch mode at a beam energy of $E = 1700 \text{ MeV}$ and 900 MeV.

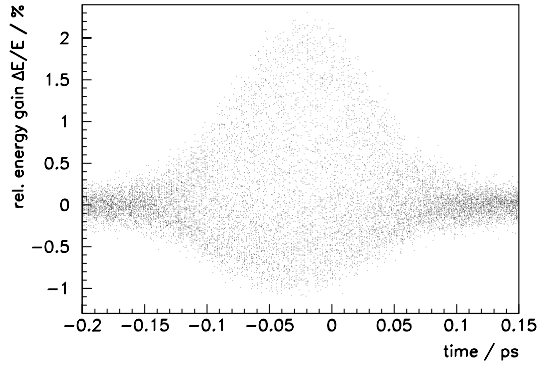


Figure 4: Distribution of electrons in time and energy after interacting with a laser pulse.

3.2 Simulation of the Laser-Electron Interaction

A numerical integration of the energy

$$\Delta E = -e c \int_{t_-}^{t_+} x'(t) \mathcal{E}(t) \sin [2\pi z(t)/\lambda_L] dt \quad (7)$$

gained or lost between the two ends of the undulator at time t_{\pm} was performed. $\mathcal{E}(t)$ is the electric field at the time-dependent electron position, and $x'(t)$ is the horizontally transverse electron velocity.

Figure 4 shows the distribution of 10^4 macro-particles in time and energy after interacting with a 400 nm laser pulse of 43 fs rms length. The following parameters were optimized numerically:

- The largest modulation amplitude was obtained for a transverse laser waist of $150 \mu\text{m}$ rms in both dimensions, given an electron waist size of $290 \times 14 \mu\text{m}$ rms.
- Detuning the undulator parameter by 1% away from the resonance value K yields the asymmetric energy distribution shown in the figure.
- The energy per laser pulse was adjusted such that a peak modulation of 2% of the beam energy was obtained.

The results for multibunch operation at 1700 MeV and at 900 MeV are shown in table 2. The repetition rate is lower than estimated before, but detuning K allows to use a larger fraction of modulated electrons. The table lists the number of electrons with $\Delta E/E > 0.5\%$. Their originally 50 fs long distribution is stretched to 170 fs rms, if the radiating device is placed 15 m away in the next straight section, assuming the present momentum compaction of $7 \cdot 10^{-4}$.

The final task is to demonstrate that synchrotron radiation from the energy-modulated electrons can be separated from the large background created by the other electrons.

E / MeV	A_L / mJ	f / kHz	$N (>0.5\%) / \text{s}^{-1}$
1700	4.0	0.25	$4.0 \cdot 10^8$
900	1.1	0.90	$1.7 \cdot 10^9$

Table 2: Simulation results for multibunch mode.

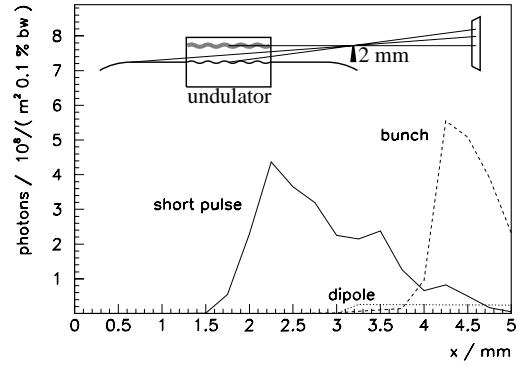


Figure 5: Radiation from energy-modulated electrons and from the other electrons of the bunch after passing a collimator edge at $x = 2 \text{ mm}$, as sketched in the figure.

3.3 Simulation of the Short Pulse Extraction

In a simulation, radiation from macro-particles randomly chosen within the distribution of figure 4 was calculated numerically, assuming a dispersion of 0.2 m at the position of a U-49 undulator ($N_u = 84$, $\lambda_u = 49 \text{ mm}$, $K = 1$).

A collimator edge was introduced 6 m downstream of the undulator center at a transverse position of 2 mm with respect to the undulator axis. The radiation hitting a screen 12 m from the undulator center is shown in figure 5. The short pulse is sufficiently separated from the bulk of radiation from other electrons. Also shown is a negligible amount of radiation from the dipole upstream of the U-49.

1-2% of background radiation are expected from off-energy electrons due to Bremsstrahlung and Touschek scattering and from non-Gaussian beam tails due to Coulomb scattering. The amount of photons from Compton scattering and fluorescence at the collimator tip is negligible. Energy-modulated electrons from previous interaction cause no background after 1-2 radiation damping times.

4 ACKNOWLEDGEMENTS

This work is funded by the Bundesministerium für Bildung, Wissenschaft, Forschung und Technologie and by the Land Berlin. Useful discussions with M. Scheer, G. Wüstefeld (BESSY-II, Berlin), W. Becker, I. Will (MBI, Berlin), B. Keil, N. Marquardt (DELTA, Dortmund), A. Zholents, M. Zoloterev (LBL, Berkeley) are gratefully acknowledged.

5 REFERENCES

- [1] E. Jaeschke: 'Status of the High Brilliance Synchrotron Light Source BESSY-II', this conference.
- [2] R.W. Schoenlein et. al.: 'Femtosecond X-ray Pulses at 0.4 Å Generated by 90° Thomson Scattering', Science Vol.274 (1996), p.236.
- [3] A.A. Zholents and M.S. Zoloterev: 'Femtosecond X-ray Pulses of Synchrotron Radiation', Phys. Rev. Lett. Vol.76, No.6 (1996), p.912.